

# Interball-2 Measurements of the Components of Thermal and Suprathermal Plasma ( $E \leq 15$ eV) in High-Latitude Regions of the Magnetosphere at Altitudes of $2-3R_E$

V. V. Afonin<sup>1</sup>, O. S. Akentieva<sup>1</sup>, and J. Smilauer<sup>2</sup>

<sup>1</sup> Space Research Institute, Russian Academy of Sciences, Profsoyuznaya ul. 84/32, Moscow, 117810 Russia

<sup>2</sup> Institute of Atmosphere Physics, Prague, Czech Republic

Received March 30, 2000

**Abstract**—The KM-7 experiment was carried out on the *Interball-2* satellite with the object of measuring the electron temperature  $T_e$  of thermal plasma in peripheral regions of the plasmasphere and in the auroral zone of the magnetosphere at altitudes of 2–3 radii of the Earth. The results of  $T_e$  measurements showed that the Maxwellian electron energy distribution, though assumed to dominate in the indicated regions when designing the apparatus, turned out to be invalid in most cases. Because of this, the current–voltage characteristics of a spherical probe were recorded and processed with the aim of checking the Maxwellian electron distribution. To this end, a numerical model was developed for the probe characteristics, as applied to the experimental conditions. The model was used to obtain, for the first time, reliable detailed data on the structure of thermal plasma in the high-latitude magnetosphere at altitudes of up to 20 000 km. The model is briefly described, and the first results are presented.

## INTRODUCTION

The KM-7 instrument was placed on the *Interball-2* satellite to measure the electron temperature  $T_e$  of thermal plasma in peripheral regions of the plasmasphere and in the auroral zone of the magnetosphere at altitudes of 2–3 radii of the Earth. Measurements were performed with the electron-temperature sensor DET-P representing a modified Langmuir probe [1].

At present, the data on the electron distribution in the above-mentioned region are scarce and restricted by the rough order-of-magnitude estimates of  $T_e$ . In designing the KM-7 instrument, it was assumed that thermal electrons are distributed in these regions according to the Maxwellian law. Since the telemetric information offered for the instrument was limited, an onboard program of data processing was developed to determine the  $T_e$  value on the basis of the above assumption. To check this assumption and to search for the regions with non-Maxwellian distribution, the current–voltage characteristics (CVCs) of the probe were also measured.

Most *Interball-2* data are the onboard-calculated  $T_e$  values conveyed through the main TM system of RTS. The CVCs were transmitted through the accessory STO TM system to the Panska Ves station, Czech Republic, only in the direct transmission regime. In this experiment, extensive information on  $T_e$  was obtained over ~2.5 years with almost continuous time overlap. The time resolution of this information was equal to either 5.12 s (about 80%) or 16 s, depending on the RTS operation mode. It contains a great deal of interesting data on the spatial–temporal  $T_e$  distribution in the region of

interest. The first data on  $T_e$  are presented in [1]. However, along with the CVCs corresponding to the Maxwellian electron distribution, there were many cases when, under certain conditions, the CVCs differed appreciably from the form corresponding to the Maxwellian distribution, so that the consistency of the experimental and calculated curves could not be achieved for any parameters of the Maxwellian thermal plasma.

An analysis of the detailed  $T_e$  variation along the spacecraft orbit made it possible to state that, in most cases, the assumption about the Maxwellian distribution of thermal plasma is invalid in the region of interest. With the aim of elucidating the real situation, the probe CVCs are analyzed in this work, and the first results on the distribution structure are presented for the thermal and suprathermal plasmas in the high-latitude region of the magnetosphere at altitudes of  $2-3R_E$ . The analysis was carried out using the probe characteristic numerical model developed for experimental conditions of KM-7. The model is not described in detail in this work, and only its main features are presented.

## MEASUREMENTS

Because of specific features of the orbit chosen, about 70% of time the spacecraft was, at least at the initial stage of flight, outside the plasmasphere in the polar magnetosphere at a height of up to ~20000 km.

Measurements were made from the instant of first switching on (August 31, 1996) to January 1999 at every switching on of the memory device of the

onboard telemetric system RTS. This made it possible to carry out practically continuous measurements for about 2.5 years; by the end of this period, the time coverage was impaired.

Contrary to the classical Langmuir probe which measures the probe current as a function of probe potential,  $I_p(U_p)$ , in our method the positive and negative bias currents are applied to the probe to measure the CVC of a floating probe (CVC-FP), namely, the floating probe potential as a function of the probe current,  $U_f(I_p)$ . This method, in fact, combines the advantages of the classical and floating probes, because it uses the floating regime and simultaneously enables one to record the CVC. The knowledge of the CVC allows one to monitor the reliability of measuring  $T_e$ , because the presence (or absence) of the Maxwellian energy distribution of electrons is monitored.

The electron temperature  $T_e$  was automatically determined aboard the spacecraft, recorded, and conveyed to the Earth in a ready-to-use (digital) form. The on-board program operation was based on the well-known fact that, for the Maxwellian distribution, the probe CVC constructed on the semilogarithmic scale contains a rectilinear portion corresponding to electron deceleration. Accordingly, the on-board program determined this rectilinear portion after taking logarithms of numerical values of the probe current (from the derivative minimum) and calculated  $T_e$  from the CVC slope.

The KM-7 instrument had two outputs, one to the onboard main RTS system and another to the auxiliary STO TM system. The CVCs were conveyed only through the STO system in the direct transmission mode, because of the deficiency of the TM quota reserved for the KM-7 instrument in the onboard RTS system.

A detailed description of the instrument and the first results of its operation, mainly according to the data of the onboard TM system, are given in [1].

When mounting the DET-P sensor, precautions were taken to reduce the influence of photoelectrons emitted from the surfaces of elements of the spacecraft construction and the sensor itself on the measurement results. As is shown in [1], these precautions were quite efficient. The effect of photoelectrons explicitly manifested itself only when the axis of spacecraft rotation deviated from its rated orientation in the perigee region, where the sensor was illuminated by solar rays. During the time period considered in this work, the perigee was in the hemisphere opposite to the region of interest.

In connection with the problem of determining the parameters of ion fluxes onto the probe (see below), the following should be pointed out. In the course of on-board processing, which requires, apart from ordinary algebraic operations, the operation of taking logarithms, the first step in measuring the CVC consisted in shifting the whole CVC in the electron current direction in order to exclude the change in sign of the analyzed quantities throughout the whole CVC. The shift-

ing was performed by applying a pseudoelectron current to the probe in such a way as to compensate for the ion current at probe potentials of  $-15$  to  $-20$  V relative to the SC. The applied pseudoelectron current is equal to the ion current onto the probe at the indicated potential values. The  $U_2$  parameter of the KM-7 instrument was also conveyed through the STO and served as an independent measure of this (ion) current. Despite the fact that this parameter was sampled too rarely and, under the conditions of fast changes in the medium parameters, did not always reflect fast variations, it may prove to be useful in determining the ion fluxes onto the probe.

### FORMULATION OF THE PROBLEM

To determine the parameters of the thermal plasma from the probe CVC, it is necessary to choose the value of the plasma parameters up to the best fit (following one or another criterion) to the experimental CVC. To make such a choice, it is necessary to know, apart from the list of adjustable plasma parameters, an analytical expression for the probe characteristic  $I_p(U_p)$ , viz., the dependence of the  $I_p$  current on the probe potential  $U_p$  relative to the plasma. Since the only available "reference" potential for every probe instrument is the potential  $U_s$  of the spacecraft mainframe relative to the plasma, it is necessary to know this value independently.

The problem of determining plasma parameters from the CVC is a complex problem even in the simplest case of isotropic thermal plasma. For the plasma moving relative to the instrument placed on the spacecraft, as occurs even if there are no intrinsic plasma motions, and especially in the presence of anisotropy and/or intrinsic plasma motions, the problem is exceedingly complicated, as becomes evident from the vast literature on this problem (see [2-4] for the corresponding bibliography). The authors of review [2] indicate that, even in the absence of a magnetic field, the problem of calculating the current collected by the probes in plasma is among the most complicated in plasma physics. Sufficiently complete solutions are known only for very simple geometries in the limits of large or small mean free paths and in the absence of motion effects.

Typically, the isotropic thermal plasma in the magnetosphere region of interest at high altitudes is characterized by seven parameters: composition (thermal electrons and ions  $H^+$ ,  $He^+$ , and  $O^+$ ), i.e., concentrations  $N_e$ ,  $N_{ij}$ ,  $j = 1-3$ , and the electron  $T_e$  and ion  $T_{ij}$ ,  $j = 1-3$ , temperatures. The composition is characterized by the ion partial concentrations  $p_{ij} = N_{ij}/N_e$  for different mass numbers  $M_{ij}$  of ions under the assumption of electro-neutrality  $N_e = \sum N_{ij}$ ,  $j = 1-3$ .

The determination of the spacecraft body potential  $U_s$  is, in essence, a problem similar to the determination of plasma parameters from the probe CVC, as applied to the whole spacecraft (see [5, 6] and, for the region of

interest, [6]). Because of this, the  $U_s$  value is included in the list of fitting parameters in the problem of determining the plasma parameters from the probe data.

The analytical expression for the probe characteristic  $I_p(U_p)$ , i.e., the probe analytical model used for determining the plasma parameters by the fitting method, is the key element and represents a problem that has not been exactly solved up to the present time [2, 7]. Three problems, solved to different degrees, exist in this field: the probe current  $I_0(U_p = 0)$  at zero potential relative to the plasma, and the probe current for the retarding ( $I(U_p < 0)$ ) and attractive ( $I(U_p > 0)$ ) potentials. The least resolved problem is the behavior of the probe current for the attractive potentials. No exact analytical expression for  $I(U_p > 0)$  suitable for practical use exists even for the simplest cases of the probe-plasma system. Only approximate expressions for certain configurations of such a system are known.

Therefore, even in the simplest case of isotropic thermal plasma, the exact determination of plasma parameters mathematically amounts to the problem of eight fitting parameters for the not necessarily correct analytical model of the object of interest. This problem is complex by itself, and it is rather problematic to attain the required accuracy. Since some pairs of parameters may correlate, the problem becomes ambiguous, and one is forced to either introduce corresponding *a priori* assumptions or independently determine one of such parameters.

Nevertheless, if the model parameters and the domains of their variation are properly chosen and if certain simplifying, though not critical for the problem investigated, assumptions are made, these expressions provide practically acceptable accuracy for fitting the parameters.

MODEL AND METHOD OF PROCESSING CURRENT-VOLTAGE CHARACTERISTICS

To analyze the CVC and determine the parameters of thermal and suprathermal plasmas in the region of interest, a numerical model was developed for the probe at the present stage. It was assumed that plasma consists of the following components:

- an isotropic thermal plasma population (one sort of the  $H^+$  ions);
- an electron beam with the energy of directed motion  $E_{eb}$  and thermal energy  $E_{etb}$ ;
- an ion beam with the energy of directed motion  $E_{ib}$  and thermal energy  $E_{itb}$ .

Figure 1 shows schematically the behavior of different probe current components as functions of the probe potential relative to the plasma. Each current component shows different potential dependences for the attractive and retarding potentials. The "electron" and "ion" curves represent the currents of the isotropic thermal plasma. The potential dependences of the electron and ion beam currents change their form (start to expo-

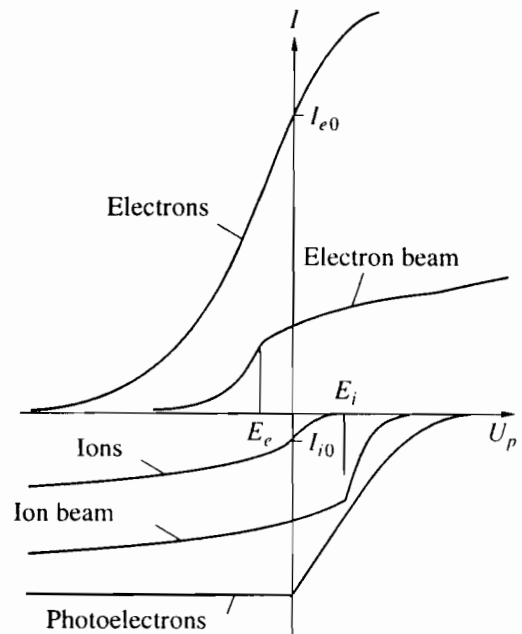


Fig. 1. Schematic representation of the behavior of various probe current components as functions of the probe potential relative to the plasma.

ponentially decay) at probe potentials exceeding (in magnitude) the energy of directed motion  $E_e$  and  $E_i$ , respectively. The photoelectron current is constant for negative potentials and exponentially decays for positive ones. The probe characteristic is a sum of the curves corresponding to the available plasma components. It is then clear that the possible CVCs of the probe are quite diversified.

The model may include the following thermal plasma components ( $E \leq 15$  eV):

- two populations of isotropic thermal plasma;
- two electron beams;
- one ion beam;
- the spacecraft body potential  $U_s$  and the plasma drift velocity  $V_d$ .

In this model, the photoelectron effect was not explicitly taken into account at the present stage, because precautions to reduce the effect of photoelectrons on the measurements, as was mentioned above, proved to be efficient enough. Nevertheless, one, probably, cannot completely exclude the effect of photoelectrons on the measurements (this issue requires a special detailed analysis). In any case, one can assert that if this effect takes place, it does not change the conclusions drawn in this work.

In addition to the above-listed parameters, the different effective collecting areas for ions and electrons, various models of the space charge layer, the spacecraft velocity  $V_s$ , and the angle of attack  $\theta$  (the angle between the direction of the Sun and the vector of plasma drift velocity  $V_d$ ) were taken into account.

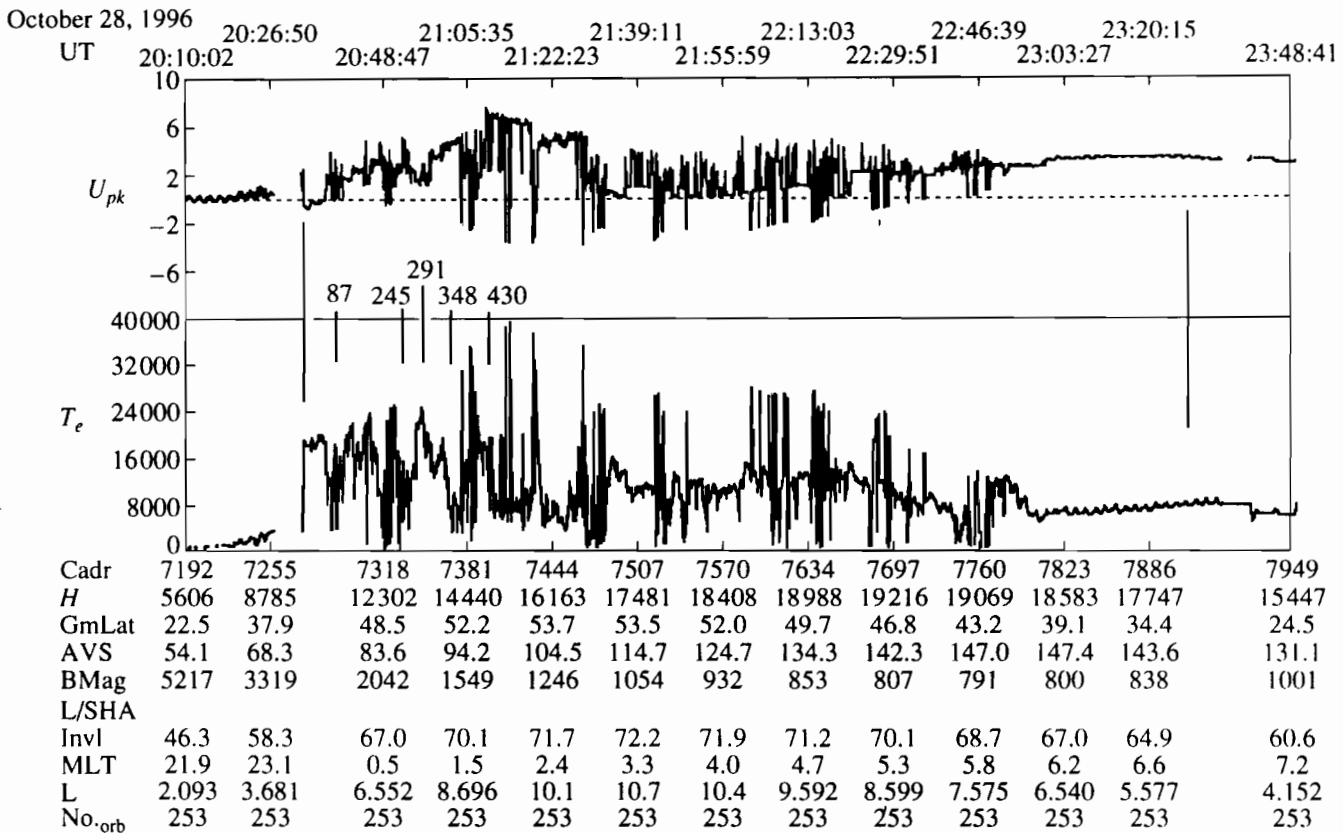


Fig. 2. Measurements of  $T_e$  and onboard  $T_e$  calculations. The period of CVC measurements and their parallel recording through the STO is indicated by vertical lines. The time moments of measuring CVCs, for which the results of processing are presented in the subsequent figures, are indicated by dashes with the corresponding CVC number.

Therefore, the numerical model of the probe includes more than 20 parameters. For this reason, the automatic determination of parameters is out of the question. It turned out that the influence of some of the parameters is appreciably weaker than the influence of the "main" parameters (electron concentration and temperature, and the beam energies). So many fitting parameters are necessary for an acceptable description of the rather complicated plasma configurations in the region of interest (two thermal populations + two electron beams + one ion beam = 2TP + 2EB + 1IB). In most cases, the plasma configuration proved to be much simpler, so that it could be described by a considerably smaller number (dependent on the particular CVC) of parameters. It also turned out that  $T_i$  and  $V_d$  have a weak effect on the results of the fitting procedure, because these parameters mainly influence the initial portion of the CVC (at the negative probe potentials). For this reason, the results were obtained by visual fitting for the lesser number of parameters, on the assumption that the isotropic plasma populations are isothermal ( $T_i = T_e$ ) and the plasma drift is absent ( $V_d = V_s$ ).

The visual fitting was carried out in the interactive regime for each particular CVC. The fitting efficiency was enhanced by the fact that for each of the four char-

acteristic parts of the probe characteristics (the acceleration and retardation portions for ions and electrons) there was an unambiguous effect of each of the main fitting parameters on the curve shape (the parameters having a weak effect on the results were excluded from the fitting procedure). The fitting procedure was performed by the summation of several curves with the known dependence on the fitting parameters and by a graphical fitting of the summarized curve to the experimental one with a visual estimate of the fitting quality.

## RESULTS

The results of measuring  $T_e$  using the onboard  $T_e$  calculation are shown in Fig. 2. The time period for which there are 1800 CVC measurements recorded in parallel through the STO is marked by the vertical lines on both sides of the diagram. At the bottom of Fig. 2, the orbital and geophysical parameters are given: the altitude  $H$ , the invariant latitude  $Invl$ , the  $L$  parameter,  $MLT$ , the  $AVS$  parameter (angle between the spacecraft velocity vector and the direction of the Sun), the magnetic field  $BMag$  in nT, and the number of the records in the file  $Cadr$ . The results of processing the CVC are presented in the subsequent figures; the moments at which the CVC were measured are indicated by the vertical

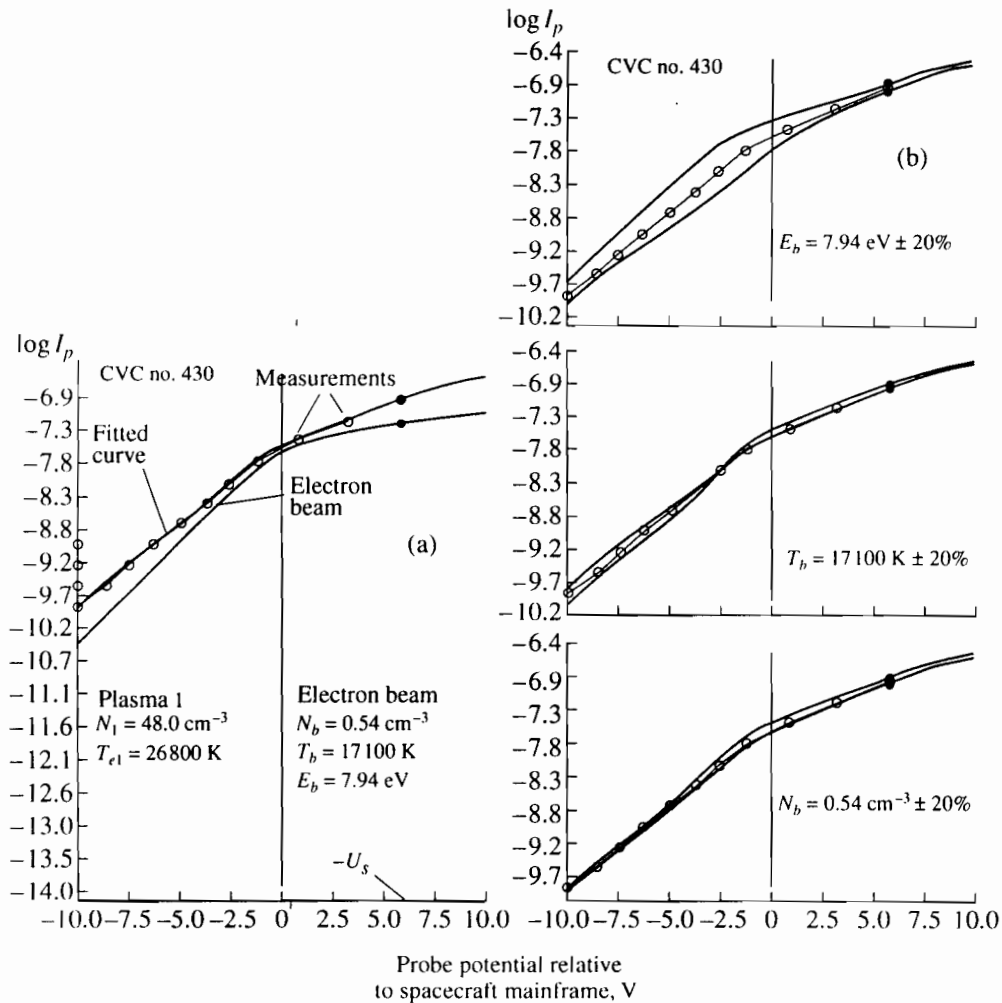


Fig. 3. (a) The result of processing CVC no. 430; (b) estimates of fitting accuracy for the electron beam parameters  $E_b$ ,  $T_b$ , and  $N_b$  for CVC no. 430.

dashes with indication of the CVC number in the communication session (Fig. 2).

Five examples of processing the CVC are presented in Figs. 3-7. All figures have the same format (except for Figs. 3b, 4) and represent the dependence of the probe current on the probe potential relative to the spacecraft mainframe. The current is given on the logarithmic scale in amperes. The upper solid line is for the model calculated probe current, and the empty circles are for the measurements of the KM-7 instrument. The dark circle corresponds to the zero potential of the DET-P sensor relative to the plasma. If there is another curve in the figure, it indicates the contribution of the electron beam to the probe current. The results of processing for all five CVCs are given in the table.

To have an idea of the fitting accuracy, Fig. 3b demonstrates the results of processing the same CVC as presented in Fig. 3a, but with variation of different parameters to within  $\pm 20\%$ . For CVC no. 87, all such estimates are presented in Fig. 4.

*Configuration of the 1TP + 1EB Plasma  
(One Isotropic Population + One Electron Beam)*

The results of the fitting procedure for the CVC no. 430 of the DET-P probe of the KM-7 instrument on the *Interball-2* are shown in Fig. 3a. The CVC was obtained on October 28, 1996, at 21:09:36 and  $H = 14903 \text{ km}$ ,  $L = 9.15$ ,  $\text{InvLat} = 70.69^\circ$ , and  $\text{MLT} = 1.71$ . The obtained CVC curve irrefutably evidences the presence of an electron beam. Indeed, the two rectilinear portions of the CVC semilogarithmic plot indicate the presence of two groups of electrons with Maxwellian distribution, the first portion (left) corresponding to the lower temperature. If this portion were a usual isotropic population, then the slopes of the rectilinear portions would be reversed: the portion close to the body potential (right) would be steeper than the next less steep (warmer) portion, which is usually referred to as the "tail" of the probe characteristic. Consequently, in this case there is a group of electrons that are colder than the main group of Maxwellian electrons, the energy distribution of the group being shifted

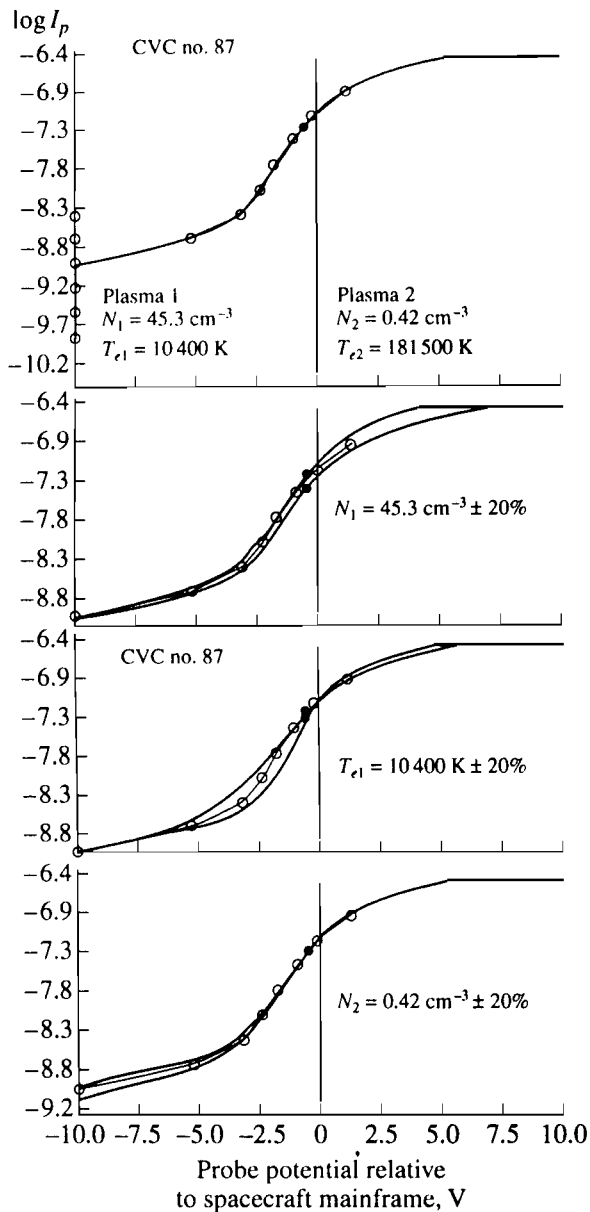


Fig. 4. The result of processing CVC no. 87 (upper panel) and estimates of fitting accuracy for  $N_1$ ,  $T_{e1}$ , and  $N_2$  (three lower panels).

by several electronvolts; i.e., this group is the electron beam.

Therefore, the thermal plasma corresponding to the measured CVC (circles) is composed of one thermal population with  $T_e = 26\,800$  K (2.3 eV) and one electron beam with a temperature  $T_{be} = 17\,100$  K (1.47 eV) lower than the temperature of the thermal population but with an energy  $E_b = 7.94$  eV of directed motion. The spacecraft body potential in this case is  $U_s = -5.9$  V. The lower curve in this case is the contribution of this beam

to the probe CVC. The bend in this curve corresponds to the energy of directed motion of the electron beam.

The fitting accuracy for the electron beam parameters is illustrated in Fig. 3b. Each of the three panels shows the same CVC as in Fig. 3a (empty circles connected by a thin line) and additionally shows two fitted probe curves obtained upon the variation of a certain parameter (indicated at each panel) by  $\pm 20\%$  relative to its chosen value.

#### *Configuration of the 2TP Plasma (Two Isotropic Thermal Populations)*

Such a plasma, composed of two isotropic thermal components with Maxwellian distributions, was observed when recording CVC no. 87 on October 28, 1996, at 20:40:19 and  $H = 11\,049$  km,  $L = 5.38$ ,  $\text{InvLat} = 64.45^\circ$ , and  $\text{MLT} = 23.93$ . The results of processing are given in the table and in the upper panel of Fig. 4. The concentrations of the warmer component constitute about 1% of the concentration of the main comparatively cold component. This does not mean that the accuracy of the parameter determination is 1%, because the contribution to the probe characteristic comes not from the concentration of this component but from its flux ( $nv$ ). In this case, the temperature  $T_{e2}$  is higher than  $T_{e1}$  by a factor of 17.

The three lower panels show, by analogy with Fig. 3b, the estimated accuracy of the fitting parameters  $N_1$ ,  $T_{e1}$ , and  $N_2$ . The accuracy of  $T_{e2}$  is not given, because both qualitatively and quantitatively it is very close to the accuracy of  $N_2$ .

#### *Configuration of the 2TP + 1EB Plasma (Two Isotropic Components + One Electron Beam)*

The plasma composed of two isotropic thermal components with Maxwellian distributions and one electron beam was observed when recording CVCs nos. 245, 291, and 348 (Figs. 5–7) on October 28, 1996, at 20:53:48, 20:57:44, and 21:02:35 UT, respectively. Other parameters were  $H = 12\,981$ ,  $13\,497$ , and  $14\,095$  km;  $L = 7.23$ ,  $7.76$ , and  $8.36$ ;  $\text{InvLat} = 68.09^\circ$ ,  $68.90^\circ$ , and  $69.73^\circ$ ; and  $\text{MLT} = 0.77$ ,  $1.01$ , and  $1.30$ , respectively. It should be noted that the energies of directed motion of electron beams are virtually the same and equal to about 5 eV. This allows them to be referred to the same magnetospheric structure, because all three CVCs are obtained within 2 degrees of the invariant latitude. Beam no. 348 is, in a sense, an anomaly, because its temperature is equal to 1600 K. Similarly, the thermal population 2 for CVC no. 291 is also different from the majority of other cases, because the concentration  $N_2$  amounts to about 50% of the  $N_1$  concentration. This ratio most often lies in the range 0.5–2%, as for CVCs nos. 245 and 348.

The discussion of geophysical aspects of these results requires a larger number of CVCs and is beyond the scope of this work. We restrict ourselves to the pre-



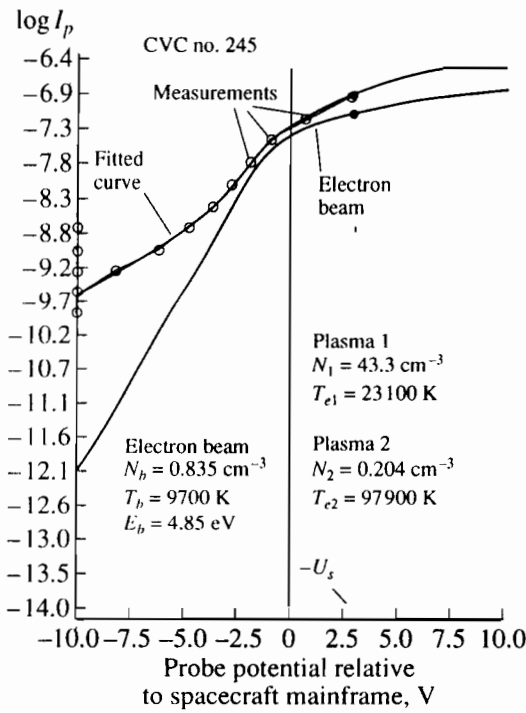


**Fig. 5.** The result of processing CVC no. 245. Concentration of the second thermal population comprises 0.5% of the concentration of the first population. The electron beam is considerably "colder" than both Maxwellian populations.

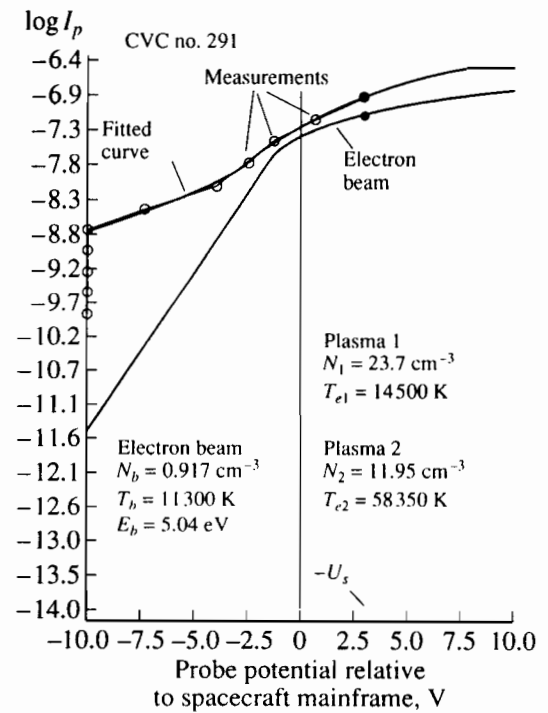


**Fig. 6.** The result of processing CVC no. 291. The concentration of the second thermal plasma population comprises 50% of the concentration of the first population.

sensation of the results of processing of the five above-mentioned CVCs.

To additionally estimate the fitting accuracy for CVC no. 430 corresponding to the configuration of the thermal plasma with one thermal population, the limiting concentrations of the second population, at which this population becomes detectable for visual fitting, are presented in the two rows below the first one. Assuming that the electron temperature of this population is  $T_{e2} = 30\,000\text{ K}$  (the  $T_2$  column), one obtains that its concentration  $N_2 < 1.0$  (the  $N_2$  column). Similarly, at  $T_{e2} = 60\,000\text{ K}$ ,  $N_2 < 0.2$ . For  $N_1 = 48.0$  this corresponds to 2 and 0.4%, respectively.

The fitting accuracy for CVC no. 87 corresponding to the plasma without electron beams is estimated in an analogous way. Assuming that the directed beam velocity corresponds to the energy  $E_{b1} = 5.0\text{ eV}$  (the  $E_{b1}$  column), one obtains that, for the thermal beam energy of  $E_{th} \approx 3\text{ eV}$  (30 000 K), the electron concentration in the beam is  $N_{b1} < 0.003\text{ cm}^{-3}$  (the  $N_{b1}$  column), otherwise it would be detectable upon the visual fitting. Similarly, for  $E_{th} \approx 0.3\text{ eV}$  (3000 K),  $N_{b1} < 0.001\text{ cm}^{-3}$ .

Thus, it follows from the results of processing CVCs that, apart from the isotropic thermal population of plasma with a Maxwellian distribution, the other components are almost always present in the high-lati-

**Table**

Figure	No. CVC	Configuration	Body potential	Thermal population 1		Thermal population 2		Electron beam		
			$U_k, \text{ V}$	$N_1, \text{ cm}^{-3}$	$T_1, \text{ K}$	$N_2, \text{ cm}^{-3}$	$T_2, \text{ K}$	$E_{b1}, \text{ eV}$	$N_{b1}, \text{ cm}^{-3}$	$T_{b1}, \text{ K}$
3a	430	1TP + 1EB	-5.9	48.0	26800	<1.0	30000	7.94	0.542	17100
4	87	2TP	+0.5	45.3	10400	0.420	181500	5.0	<0.003	30000
						<0.2	60000	5.0	<0.001	3000
5	245	2TP + 1EB	-2.8	43.4	23100	0.204	97900	4.85	0.835	9700
6	291	2TP + 1EB	-3.0	23.7	14500	11.95	58350	5.04	0.917	11300
7	348	2TP + 1EB	-0.4	23.0	16300	0.114	177500	4.93	0.037	1600

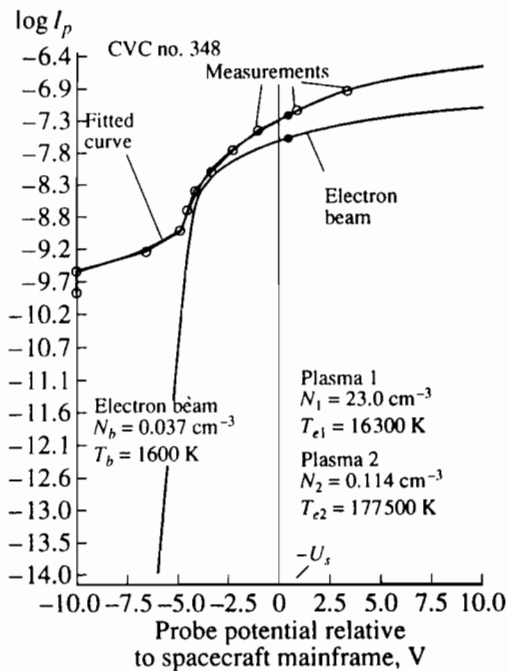


Fig. 7. The result of processing CVC no. 348. An example of an anomalously "cold" beam.

tude magnetosphere at altitudes of 10–20 thousand km: a warmer thermal plasma with Maxwellian distribution, electron beams with various ratios of the thermal and directed velocities, or the ion fluxes additional to the plasma thermal populations.

While the method used made it possible to determine the main electron beam parameters, such as  $N$ ,  $E$ , and  $T_e$ , with an acceptable accuracy, only the presence of the above-mentioned additional ion fluxes can, at most, be reliably stated at present. Because of the specific features of the formation of the total probe current characteristic, reliable determination of the additional ion flux seems to be impossible without invoking auxiliary information. In some cases, this becomes possible with the use of the  $U_2$  parameter of the KM-7 instrument. However, this issue is beyond the scope of this work.

### CONCLUSIONS

The following results are obtained from the analysis of the CVCs based on the data of two passes.

(1) The isotropic thermal plasma population with a Maxwellian distribution and without an admixture of other components of thermal or suprathermal plasma is practically absent in the high-latitude magnetosphere at altitudes of  $\sim 10000$ – $20000$  km. The thermal plasma

actually observed in these spatial regions is almost always composed of various combinations of Maxwellian and non-Maxwellian components.

(2) The following components of thermal and suprathermal plasma electrons and ions with energies  $E \leq 15$  eV were revealed.

—An isotropic population of electrons and ions with Maxwellian distributions.

—Electron beams with various ratios of the thermal and directed energies. The beams with directed motion energy  $E_b$  much greater than their thermal energy  $E_{th}$  ("cold" electron beams) are most frequently observed. However, the beams with an approximately equal ratio of thermal and directed energies ("hot" electron beams) are also observed. The absolute values and the ratio of the directed and thermal electron beam energies indicate the region and, possibly, the mechanism of their formation.

—The additional ion fluxes. Only their existence can be reliably stated at present. This can easily be seen from even visual inspection of the CVC forms in the negative potential range. Additional analysis is required to reveal the possibility of determining their parameters and to reveal whether they are isotropic or directed. It is conceivable that we have to do with a significant contribution ( $n_i v_i$ ) of suprathermal ions.

### REFERENCES

1. Afonin, V.V., Akentieva, O.S., Smilauer, J., and Simunek, I., First Results of Thermal Plasma Measurements in the *Auroral Probe* Mission (Experiment KM-7), *Kosm. Issled.*, 1998, vol. 36, no. 1, pp. 16–32.
2. Laframboise, J.G. and Sonner, L.J., Current Collection by Probes and Electrodes in Space Magnetoplasmas: A Review, *J. Geophys. Res.*, 1993, vol. 98, pp. 337–357.
3. Parker, L.W. and Whipple, E.C., Jr., Theory of Spacecraft Sheath Structure, Potential, and Velocity Effects on Ion Measurements by Traps and Mass Spectrometers, *J. Geophys. Res.*, 1970, vol. 75, pp. 4720–4733.
4. Medicus, G., Spherical Langmuir Probe in "Drifting" and "Accelerated" Maxwellian Distribution, *J. Appl. Phys.*, 1962, vol. 33, no. 10, pp. 3094–3100.
5. Whipple, E.C., The Equilibrium Potential of a Body in the Upper Atmosphere and in Interplanetary Space, *NASA Report X-615-65-296*, Greenbelt, Md: Goddard Space Flight Center, 1965.
6. Spacecraft/Plasma Interactions and Their Influence on Field and Particle Measurements, *Proc. 17th ESLAB Symp., Noordwijk, Netherlands, Sept. 1983, ESA SP-198*, European Space Agency, 1983.
7. Kozlov, O.V., *Elektricheskii zond v plazme* (Electric Probe in Plasma), Moscow: Atomizdat, 1969.